Follow us @BoneJointRes

Freely available online OPEN ACCESS

BJR

BONE FRACTURE

High slew rate pulsed electromagnetic field enhances bone consolidation and shortens daily treatment duration in distraction osteogenesis

Y. Li,
Y. Yang,
M. Wang,
X. Zhang,
S. Bai,
X. Lu,
Y. Li,
E. I. Waldorff,
N. Zhang,
W. Y-W. Lee,
G. Li

From The Chinese University of Hong Kong, Hong Kong, China

Aims

Distraction osteogenesis (DO) is a useful orthopaedic procedure employed to lengthen and reshape bones by stimulating bone formation through controlled slow stretching force. Despite its promising applications, difficulties are still encountered. Our previous study demonstrated that pulsed electromagnetic field (PEMF) treatment significantly enhances bone mineralization and neovascularization, suggesting its potential application. The current study compared a new, high slew rate (HSR) PEMF signal, with different treatment durations, with the standard Food and Drug Administration (FDA)-approved signal, to determine if HSR PEMF is a better alternative for bone formation augmentation.

Methods

The effects of a HSR PEMF signal with three daily treatment durations (0.5, one, and three hours/day) were investigated in an established rat DO model with comparison of an FDA-approved classic signal (three hrs/day). PEMF treatments were applied to the rats daily for 35 days, starting from the distraction phase until termination. Radiography, micro-CT (μCT), biomechanical tests, and histological examinations were employed to evaluate the quality of bone formation.

Results

All rats tolerated the treatment well and no obvious adverse effects were found. By comparison, the HSR signal (three hrs/day) treatment group achieved the best healing outcome, in that endochondral ossification and bone consolidation were enhanced. In addition, HSR signal treatment (one hr/day) had similar effects to treatment using the classic signal (three hrs/day), indicating that treatment duration could be significantly shortened with the HSR signal.

Conclusion

HSR signal may significantly enhance bone formation and shorten daily treatment duration in DO, making it a potential candidate for a new clinical protocol for patients undergoing DO treatments.

Cite this article: *Bone Joint Res* 2021;10(12):767–779.

Keywords: Pulsed electromagnetic field, Distraction osteogenesis, Bone formation

Article focus

- To evaluate the effects of a novel high slew rate (HSR) pulsed electromagnetic field (PEMF) signal on distraction osteogenesis (DO).
- To compare the new HSR PEMF treatment on bone formation with the FDA-approved classic PEMF signal in DO.
- To investigate the biological mechanisms of PEMF in augmenting bone formation in DO.

Correspondence should be sent to Gang Li; email: gangli@cuhk.edu.hk

doi: 10.1302/2046-3758.1012.BJR-2021-0274.R1

Bone Joint Res 2021;10(12):767–779.

Key messages

- HSR PEMF treatment enhanced bone consolidation process, compared to no treatment and classic signal treatment in DO.
- In contrast to classic PEMF treatment (three hrs/day), HSR PEMF treatment (one hr/day) achieved similar promoting effects on bone formation.

Strengths and limitations

- This was a comprehensive study, investigating the therapeutic effects of HSR PEMF with varying duration at different stages of bone healing in DO.
- HSR PEMF signal showed stronger promoting effects on chondrogenesis and bone mineralization than that of a classic PEMF in DO, providing a potential new clinical choice for PEMF treatment.
- Despite the fact that the rat DO model has been well established and used for many studies, it may not reflect the real clinical situation of DO in humans.
- Future clinical trials are needed to verify the current findings.

Introduction

Distraction osteogenesis (DO) is a useful orthopaedic procedure commonly used to lengthen and reshape bones by stimulating bone formation using controlled slow mechanical stretching.[1-3] Initially reported by Ilizarov in 1989,[1] DO has been widely accepted and applied in orthopaedics and traumatology surgeries. The last two decades have led to great advancement of DO, and DO techniques are now widely applied to treat difficult orthopaedic conditions, such as limb deformities,[4] nonunion,[5] and segmental bone defects.[6] DO surgery is usually applied as the last resort when other attempts have failed to increase limb salvage and functional recovery, and improve life quality.[7] Successful DO clinical treatment outcomes rely on many factors such as adequate blood supply and adaptation of surrounding soft-tissues to the mechanical stretching.[2,3] Patient physique and treatment duration affect bone-healing in DO, and are associated with complications. Complications such as delayed bone-healing during DO exist to a certain extent; efforts towards developing novel strategies to improve bone formation/consolidation and shorten the DO treatment duration continue.[8-12]

Pulsed electromagnetic fields (PEMFs), as noninvasive physical stimuli that have been proven to promote bone repair, represent a new biophysical treatment solution with greater convenience and less complication.[13-18] After the PEMF treatment for promoting bone repair was approved by the USA Food and Drug Administration (FDA), various PEMF signals have been investigated for possible clinical applications.[19-26] It is now clear that PEMF promotes bone-healing by enhancing osteogenesis[27,28] and angiogenesis.[29,30] The promoting effects of PEMF are signal-specific and dependent.[14,15] Therefore, careful investigation of a specific PEMF signal should be conducted before it may be clinically applied. Discussion of the diverse effects of PEMFs with different parameters has continued since PEMF was first introduced into the field of physiotherapy.[27,31] Slew rate is one of the signal parameters, defined as the rate of B field change over time (dB/dt). PEMF signals of various slew rates reduce trabecular bone loss differently in the proximal tibia in skeletally mature osteoporotic rats.[32] We previously showed that a novel PEMF signal with relatively high slew rate significantly enhanced bone mineralization and neovascularization.[30] This high slew rate PEMF signal revealed supreme efficiency and effectiveness in promoting bone mineralization, indicative of its promising therapeutic potential that may clinically benefit patients even more compared to the classic FDA-approved signals.

In the current study, a specific HSR PEMF signal of the same waveform and frequency was derived from the FDA-approved signal, Physio-Stim (Orthofix Medical, USA).[33] We then evaluated the effects of this HSR PEMF signal with three different treatment durations on bone formation in comparison to the FDA-approved signal. The current study brings more insights into the biological mechanisms of HSR PEMF in augmenting bone formation in DO, and may provide guidance for optimizing PEMF treatment protocols for clinical applications.

Table I. Pulsed electromagnetic field treatment conditions.

Group	Treatment
G_{con}	Lengthening and no PEMF treatment
$G_{classic3h}$	Lengthening and PEMF treatment with classic signal (3 hrs/day)
$G_{HSR1/2h}$	Lengthening and PEMF treatment with HSR signal (30 mins/day)
G_{HSR1h}	Lengthening and PEMF treatment with HSR signal (1 hr/day)
G_{HSR3h}	Lengthening and PEMF treatment with HSR signal (3 hrs/day)

PEMF classic signal (10 T/s, Physio-Stim).PEMF classic signal (10 T/s, Physio-Stim).
PEMF HSR signal (a derivative of the Physio-Stim with a higher slew rate).
N = 18 rats per group (n = 6 terminated at day 28, 42, and 56 as shown in workflow of the experimental plan).
HSR, high slew rate; PEMF, pulsed electromagnetic field.

Methods

All experiments were approved by the Animal Research Ethics Committee of the Chinese University of Hong Kong (AEEC number: 20-225-MIS). We have included an ARRIVE checklist to show that we have conformed to the ARRIVE guidelines. The sample size was calculated based on our pilot study wherein we compared classic signal with HSR signal, with the same daily treatment duration of three hours per day. The micro-CT (μCT) analysis revealed the mean BV/TV outcome as 0.453 (standard deviation (SD) 0.025) in classic signal versus 0.515 (SD 0.041). Using power calculation with a probability of 90%, we estimated the required sample size to be six rats per group per timepoint.

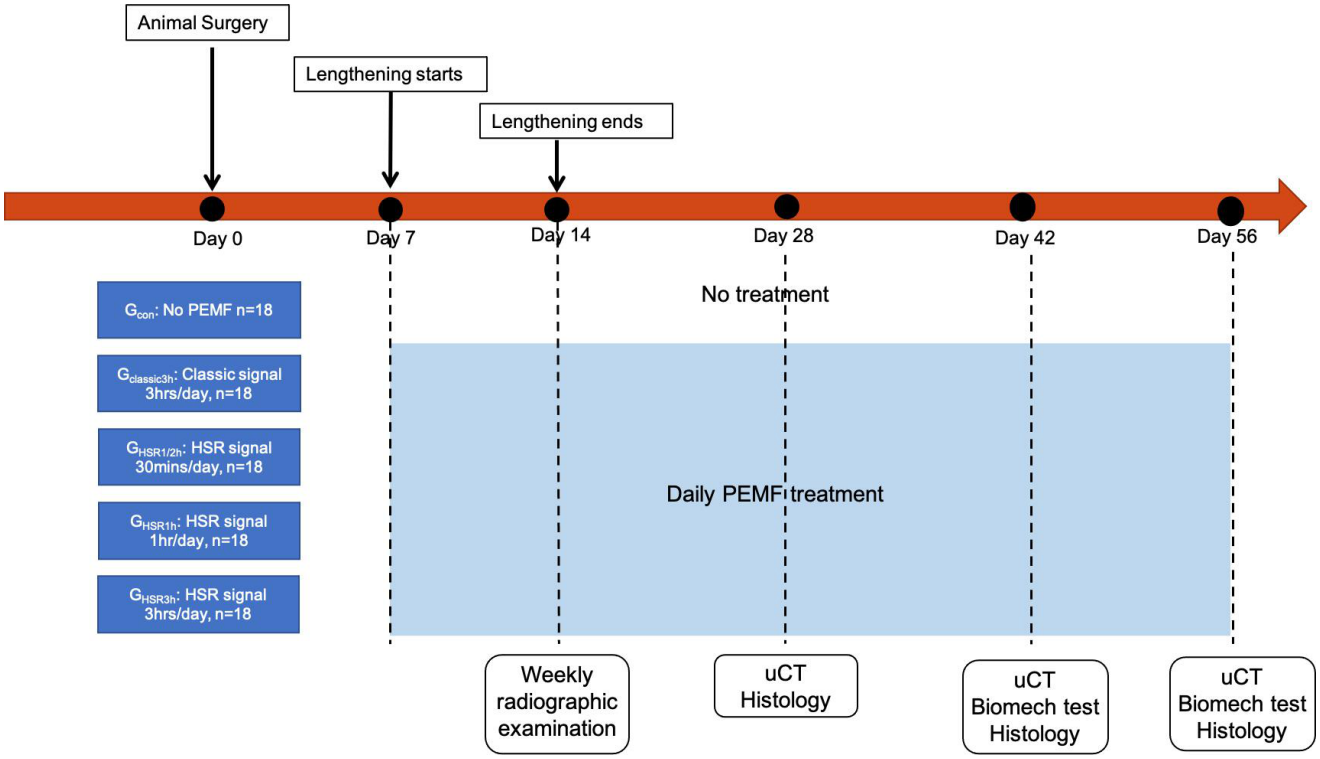

Fig. 1

Workflow of experimental plan. HSR, high slew rate; PEMF, pulsed electromagnetic field; μCT, micro-CT.

PEMF signals. One classic FDA approved signal and one HSR signal were used in this study. The classic signal (Physio-Stim, Orthofix) has been approved by the USA FDA for healing of long-bone nonunions,[33] and has been commercialized as one of the current clinical standards for the PEMF treatment of long-bone nonunions. Treatment regime was determined based on clinical conditions (fracture nonunions) where it is applied three hours per day until healing has been achieved.[33] The Physio-Stim PEMF signal has a fundamental burst frequency of 15 Hz, pulse frequency of 3.85 kHz, and slew rate of 10 T/s. The HSR signal (Orthofix Medical) has the same burst and pulse frequencies but a higher slew rate, theoretically resulting in a higher energy input to the target tissue.[32] The HSR signal was compared with the classic signal for the effects on bone formation and condition in an established rat DO model.

Animal surgery and distraction osteogenesis protocol. A total of 90 Sprague-Dawley (SD) rats (12-week-old, male, mean weight 280.19 g (SD 15.13)) were used. After being anaesthetized with intraperitoneal injection of 0.2% (v/v) xylazine and 1% (v/v) ketamine in phosphate-buffered saline (PBS), all animals were subjected to a right tibia transverse osteotomy procedure at the mid-shaft near the fibula-tibia junction under sterile condition as previously described.[30] An external fixator was applied to fix proximal and distal segments of the osteotomy site. An osteotomy was also made in the right fibula. Surgical incisions were then sutured sequentially. All rats were randomized into five groups with 18 in each group (Table I). All groups had bone lengthening started at day seven postoperatively with 0.375 mm increments every 12 hours, twice a day for seven days, for a total lengthening distance of 5.25 mm. Animal wellbeing and condition of surgical site were checked every three days. No infection or other complications of rats were observed. All rats were included for data analysis.

In vivo PEMF exposure. In the five randomized groups, different PEMF treatments were applied (Table I). In $G_{classic3h}$, $G_{HSR1/2h}$, G_{HSR1h}, and G_{HSR3h}, rats received daily PEMF treatment from day seven postoperatively (i.e. once lengthening had been completed) until termination. Detailed treatment conditions are shown in Table I. The PEMF treatment was given to rats using our established protocol[30] with a specialized in vivo PEMF device (Orthofix Medical). Rats placed under the same condition but without PEMF exposure served as the control group (G_{con}). Workflow of the experimental plan is shown in Figure 1.

To minimize potential confounders, all animals received daily treatments simultaneously, and rats from the control group were kept in a nonoperating PEMF device during the treatment duration. Group allocation and randomization were performed by YY, treatment was performed by YY and MW, and outcome assessment and data analysis were processed by YL, XL, and SB blindly in a random order. Weekly radiograph examination, including the lengthening zone, was taken until termination to record the trend of bone regeneration and consolidation.

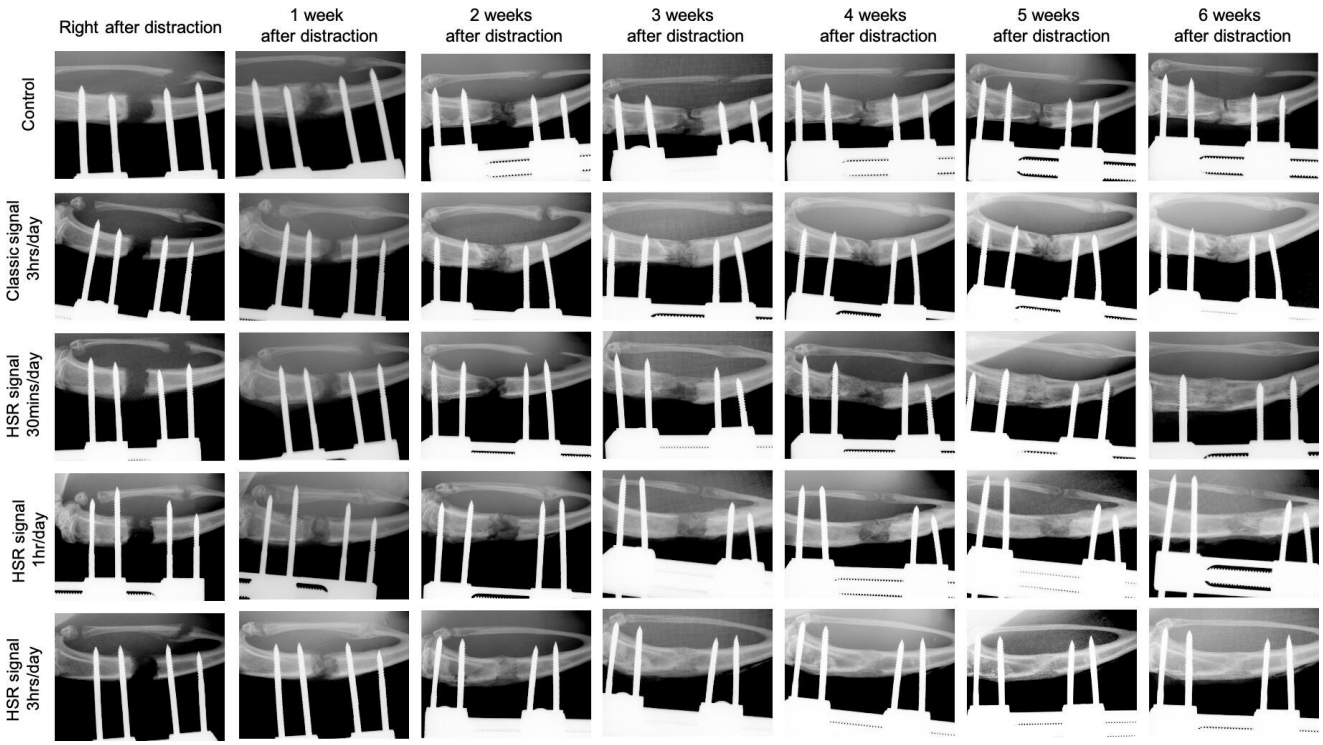

Fig. 2

Radiological assessment results. At the end of lengthening, a weekly anteroposterior radiograph including the distraction zone was taken until termination. Representative series of radiographs across the duration of distraction osteogenesis (DO) showed the progression of bone consolidation. All pulsed electromagnetic field (PEMF) treatments had different levels of promoting effects on callus formation. GHSR3h appeared to have the best bone-healing outcome with earlier continuous callus formation and better consolidation. Gclassic3h and GHSR1h appeared to have a similar healing outcome, which was better than those of GHSR1/2h and Gcon, but not as good as GHSR3h. HSR, high slew rate.

After termination at two, four, and six weeks after lengthening, tibia samples were immediately subjected to μCT analysis, mechanical testing and histomorphometry, and immunohistochemistry staining to determine the quality of the regenerated bone.

Digital radiographs. After the lengthening phase, a weekly anteroposterior (AP) radiograph including the lengthening zone was taken until termination using a digital X-ray machine (MX-20, Faxitron X-Ray, USA) under an exposure time of 6,000 ms and a voltage of 32 kV.

Micro-CT. The bone formation within the lengthening zone was quantitatively assessed with μCT (n = 6/group/timepoint). Briefly, all the specimens were imaged using a high-resolution μCT (Viva-CT40, Scanco Medical, Switzerland) with a voltage of 70 kV and a current of 114 μA. 3D images of mineralized callus were constructed, and a Gaussian filter (sigma = 0.8, support = 2) was used to suppress noise. Sagittal images of the distraction zone were used to facilitate selection of regions of interest (ROIs) for analysis. Calcified callus was constructed using thresholds between 211 and 1,000, and uncalcified callus was constructed using thresholds between 158 and 211. The central 130 slides of the distraction site in horizontal plane were selected as the region of interest. Bone volume/total tissue volume (BV/TV) of the calcified, uncalcified, and total callus, and bone mineral density (BMD) of calcified callus in each specimen were analyzed.

Four-point bending mechanical testing. A mechanical test was performed on the freshly isolated specimens immediately after termination on four weeks and six weeks after distraction (n = 6/group/timepoint). The contralateral tibia was tested as an internal control. A four-point bending device (H25KS; Hounsfield Test Equipment, UK) with a 250 N load cell was used to test the tibia to failure. The tibiae were loaded in the AP direction with the inner and outer span of the blades set at 8 mm and 18 mm, respectively. The long axis of the tibia was placed perpendicular to the blades during the test. The modulus of elasticity (E-modulus), ultimate load, and energy to failure were obtained and analyzed with built-in software (QMAT Professional; Tinius Olsen, USA). The biomechanical properties of the new bone were expressed as percentages of the contralateral intact bone.

Histomorphometry and immunohistochemistry staining. All tibiae were fixed in 10% formalin for 24 hours at room temperature and then subjected to decalcification in 10% ethylenediaminetetraacetic acid (EDTA) solution (pH 7.2) for three weeks with intermittent shaking before embedding in paraffin; 7 μm sections were cut by a rotary microtome (HM 355 S, ThermoFisher Scientific, Germany) along the long axis of each tibia in the sagittal plane. After deparaffinization, haematoxylin and eosin (H&E) staining, Goldner's Trichrome staining, and immunohistochemistry staining were performed.

Immunohistochemistry staining was performed using a standard protocol. Sections were treated with primary antibodies to rabbit anti-rat collagen type I (Col I; Abcam, UK, ab34710, 1:100) and rabbit anti-rat osteocalcin (OCN; Santa Cruz Biotechnology, USA, 1:100, sc-365797) overnight at 4°C; a horseradish peroxidase-streptavidin detection system (Dako, USA) was used, followed by counterstaining with haematoxylin. Five randomly selected pictures from each section taken at 100× magnification were used for semiquantitative analysis. Percentage of positive area was analyzed using ImageJ (National Institutes of Health, USA).

Statistical analysis. All quantitative data were analyzed using SPSS v18.0 software for windows (SPSS, USA). One-way analysis of variance (ANOVA) and Tukey's multi-comparison test were used for comparison of mean values. A p-value < 0.05 was considered statistically significant.

Results

Radiological assessment of the distraction regenerate site. Representative serial radiographs across the time course of DO showed the progression of bone consolidation (Figure 2). Overall, radiograph results showed that all PEMF treatments had different levels of promoting effects on callus formation, with G_{HSR3h} appearing to have the best bone-healing outcome. Continuous callus with no visible gap in the distraction regenerate site appeared much earlier in G_{HSR3h} compared to other groups, and almost all callus were consolidated at week 5 after lengthening and there were signs of bone-remodelling. $G_{classic3h}$ and G_{HSR1h} appeared to have a similar healing outcome, which was better than those of G_{con} and $G_{HSR1/2h}$, but not as good as G_{HSR3h}.

Micro-CT assessment of the distraction site. Representative μCT images from two, four, and six weeks after lengthening are shown in Figure 3. Two weeks after lengthening and treatment with the HSR signal three hrs/day, G_{HSR3h} significantly promoted callus formation compared to all four other groups. Volumes of uncalcified and calcified bone and mineral density of the callus were significantly higher in G_{HSR3h} (Figure 4a). The other three PEMF treatment groups also revealed some levels of promoting effects on callus formation. Compared with G_{con}, no significant difference in calcified BV/TV was observed in $G_{classic3h}$, $G_{HSR1/2h}$, and G_{HSR1h}, yet total BV/TV was significantly higher in $G_{classic3h}$ and G_{HSR1h} compared to G_{con}. After four and six weeks of lengthening, G_{HSR3h} still had the best bone-healing outcome, with significantly higher bone volume and greatest BMD (Figures 4b and 4c). No significant difference was seen between $G_{classic3h}$ and G_{HSR1h}. Interestingly, in all HSR PEMF treatment groups the longer the treatment duration, the more calcified bone was found in the distraction regenerate site, suggesting that HSR signal enhances bone-healing by promoting mineralization. Total BV/TV in $G_{classic3h}$, G_{HSR1h}, and G_{HSR3h} was significantly higher than that of G_{con}, but no difference was seen at four and six weeks between $G_{classic3h}$, G_{HSR1h}, and G_{HSR3h}.

Mechanical testing. The results of four-point bending mechanical testing at four and six weeks after lengthening showed that the mechanical properties in almost all of the PEMF groups were significantly improved compared to the non PEMF control, except in the $G_{HSR1/2h}$ where the ultimate load at weeks 4 and 6, and E-modulus at week 6, were statistically similar to G_{con} (Figure 5). At week 4, the ultimate load, energy to failure, and elastic modulus of the new formed bone in G_{HSR3h} were all significantly greater than those of the other four groups, except the ultimate load in G_{HSR1h}. At week 6, the significant energy to failure superiority of G_{HSR3h} over the other four groups remained. However, the ultimate load and elastic modulus of G_{HSR3h} were only significantly better than those in G_{con} and $G_{HSR1/2h}$. At both timepoints, although the mechanical properties in both $G_{classic3h}$ and G_{HSR1h} were always significantly better than those in the G_{con}, no statistically significant differences were seen between these two groups.

Histology and immunohistochemistry staining. H&E and Goldner's Trichrome staining were used to investigate the histomorphometry of the newly formed bone. Immunohistochemistry (IHC) staining of OCN and collagen type I were used to investigate osteogenic activity and quality of the newly formed bone callus. Two weeks after lengthening, in G_{con} and $G_{HSR1/2h}$, bone defects in the distraction site were mostly covered by fibrous tissue, with few instances of newly formed cartilage and bone (Figures 6 and 7). In $G_{classic3h}$ and G_{HSR1h}, small amounts of hyaline cartilage were found inside the distraction regenerate site, indicating that bone formation already started with endochondral ossification. In contrast, the bone formation was accelerated in G_{HSR3h}, where a large amount of hyaline cartilage appeared within the distraction regenerate site, and osteoids were partially mineralized inside the newly formed bone. IHC staining of OCN indicated that all PEMF treatments had different levels of promoting effects on OCN expression, and G_{HSR3h} appeared to have the most increased expression of OCN.

Four weeks after lengthening, all five groups were at bone formation phase with endochondral ossification inside the distraction regenerate site (Figure 8). In G_{con} and $G_{HSR1/2h}$, large amount of fibrous tissues still remained inside the bone defect site, whereas most of the soft tissues had been replaced by hyaline cartilage in $G_{classic3h}$ and G_{HSR1h}. In G_{HSR3h}, percentage of hyaline cartilage started to decrease compared with that of week 2, and the amount of calcified bone significantly increased compared to other PEMF treatment groups. The level of expression of OCN remained similar to that of week 2, G_{HSR3h} still had the most abundant OCN expression in the distraction regenerate site. Six weeks after lengthening, in $G_{classic3h}$, $G_{HSR1/2h}$, and G_{HSR1h}, endochondral ossification and callus formation in the middle of the distraction regenerate were still ongoing with signs of bone-remodelling, whereas relatively larger amounts of fibrous tissues and soft callus were still seen in the distraction regenerate site

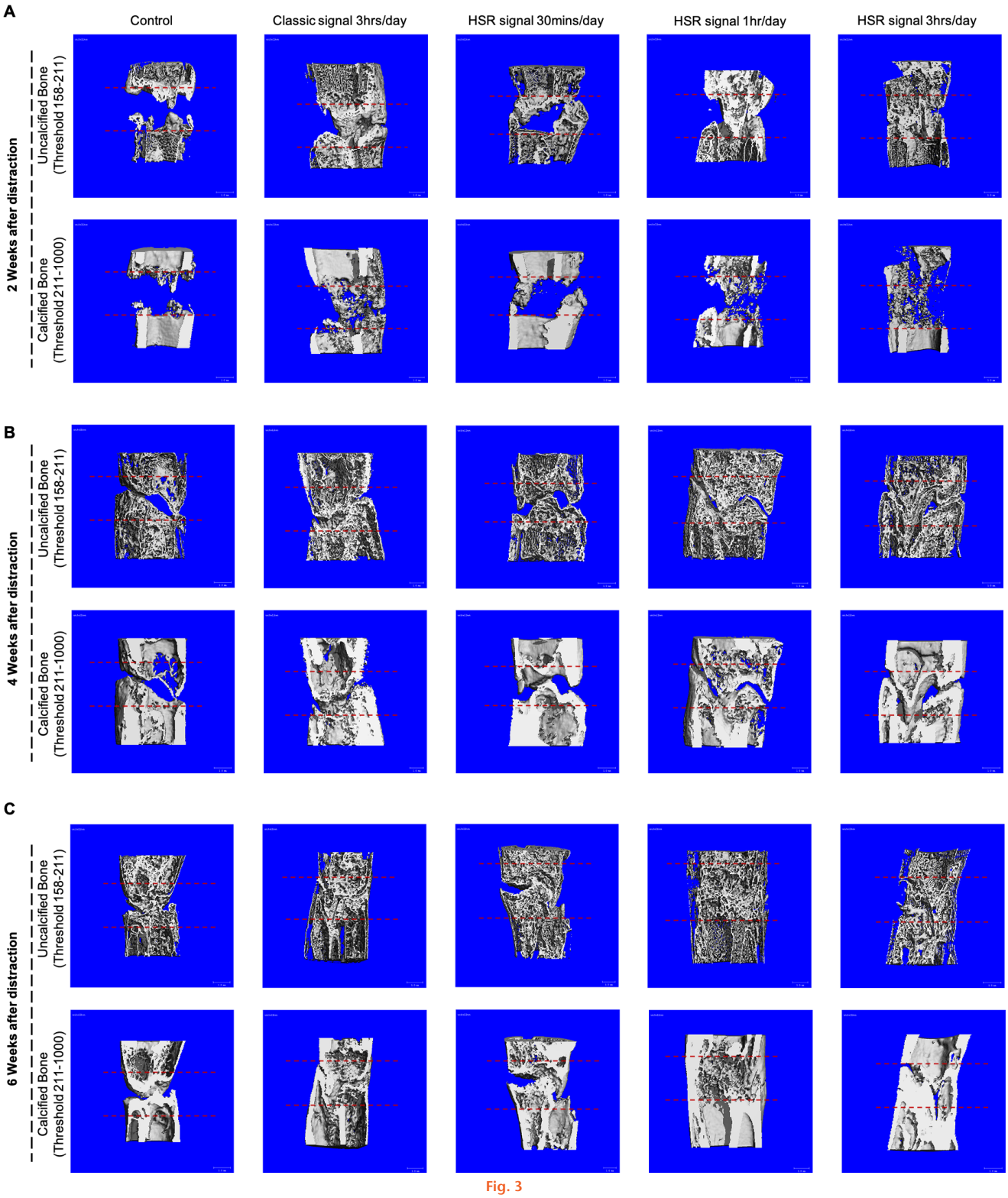

Fig. 3

Micro-CT (μCT) analysis of distraction site. Representative pictures reconstructed by μCT at a) two weeks, b) four weeks, and c) six weeks after distraction.HSR, high slew rate.

in G_{con}. In contrast, endochondral ossification was mostly complete and bone-remodelling was partially complete in G_{HSR3h} (Figures 9 and 10). IHC staining of OCN indicated that OCN expression was still strong in $G_{classic3h}$, G_{HSR1h}, and G_{HSR3h}. The highest expression level of Col I was seen in G_{HSR3h}, indicating that PEMF treatment with HSR

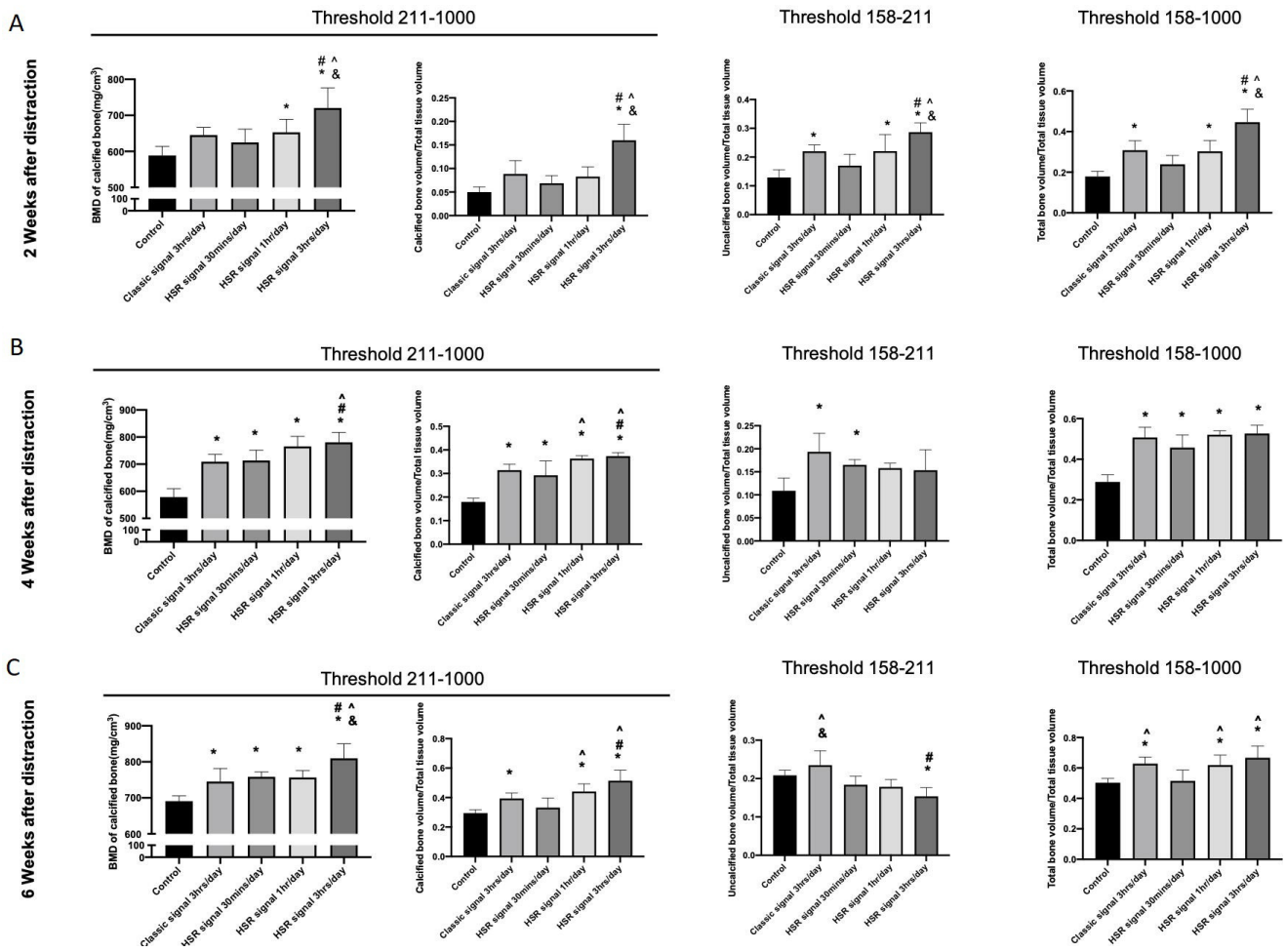

Fig. 4

Analysis data of distraction site after distraction are demonstrated at a) wo weeks, b) four weeks, and c) six weeks after distraction. Attenuation above 211 represented fully calcified bone callus, and attenuation between 158 and 211 represented the new uncalcified callus. Two weeks after lengthening, callus formation was significantly promoted in GHSR3h, with increased volume of uncalcified and calcified bone and mineral density of the callus compared with other groups. All three other pulsed electromagnetic field (PEMF) treatment groups also revealed some levels of promoting effects on callus formation. On four and six weeks after lengthening, GHSR3h still had the best bone-healing outcome, with significantly higher bone volume and bigger bone mineral density (BMD). Classic signal three hrs/day (Gclassic3h) and HSR signal 1 hr/day (GHSR1h) appeared to have a similar healing outcome, which was better than those of GHSR1/2h and Gcon, but not as good as GHSR3h. * vs control (Gcon), "#" vs Gclassic3h, "^" vs high slew rate (HSR) signal 30 mins/day (GHSR1/2h), "&" vs GHSR1h, $p < 0.050$. One-way analysis of variance and Tukey's multi-comparison test were used for comparison of mean values.

signal (3 hrs/day) achieved the best quality of new bone formation.

Discussion

The current study examined the effects of therapeutic PEMF signals with different treatment conditions on bone-healing in an established rat DO model. Overall, treatment using HSR signal (three hrs/day) achieved the best healing outcome. This treatment protocol promoted chondrogenesis and callus formation at the early stage of bone-healing (two weeks after lengthening), and enhanced bone mineralization and consolidation at the middle and late stage of healing (four and six weeks after lengthening). The quality of new regenerates was also improved in this group, in comparison to the classic PEMF signal. The HSR signal had accelerated endochondral ossification, bone formation, and bone-remodelling when applied for three hrs/day. The quicker hyaline cartilage formation at the early stage of lengthening phase and callus mineralization suggested that the effects of HSR signal might be different from the classic PEMF signal, which showed a mild promoting effect on all aspects during bone-healing. HSR signal treatment shortened the bone-healing process, in that endochondral ossification was fastened. At six weeks after lengthening, the bone-remodelling was almost complete in the G_{HSR3h} (HSR signal, three hrs/day) treatment group, whereas the bone formation in all other groups was still ongoing.

In comparison with $G_{classic3h}$ and G_{HSR1h}, treatment with HSR signal at one hr/day achieved similar healing outcome as treatment with the classic signal at three hrs/day. This indicates that the HSR signal could significantly shorten the treatment duration (from three hrs/day to one hr/day), which may be beneficial for clinical use (for

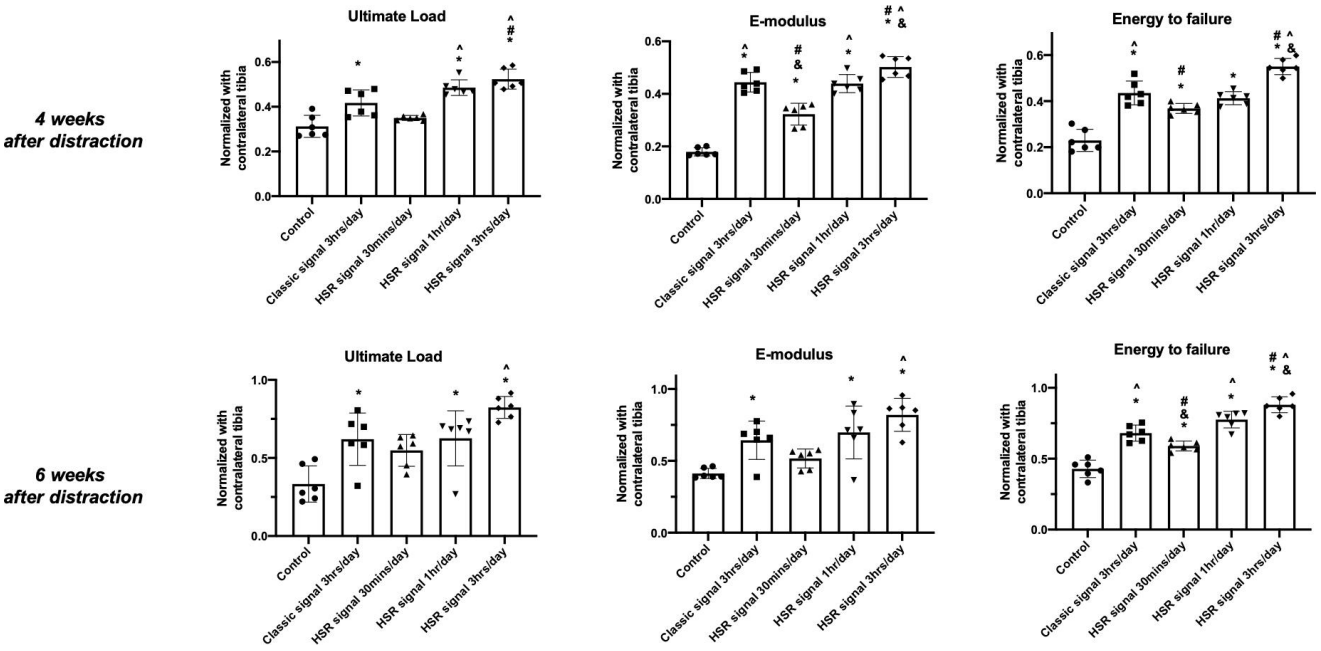

Fig. 5

Four-point bending mechanical testing results in E-modulus, ultimate load, and energy to failure on weeks 4 and 6 after distraction. The results showed a significant improvement in mechanical properties in GHSR3h. After being normalized to the contralateral intact tibia, ultimate load, energy to failure, and elastic modulus of the newly formed bone were all significantly increased compared to other groups. The mechanical properties of the new bone in Gclassic3h and GHSR1h were also enhanced compared to GHSR1/2h and Gcon, and no statistical difference was found between GHSR1/2h and Gcon. * vs control (Gcon), "#" vs classic signal three hrs/day (Gclassic3h), "^" vs high slew rate (HSR) signal 30 mins/day (GHSR1/2h), "&" vs HSR signal one hr/day (GHSR1h), $p < 0.050$. One-way analysis of variance and Tukey's multi-comparison test were used for comparison of mean values.

example, to increase the patient's compliance). On week 4 after lengthening, the amount of cartilage formation in G_{HSR1h} was significantly more than that in $G_{classic3h}$ ($p < 0.001$, one-way ANOVA and Tukey's multi-comparison test), whereas the amount of calcified bone remained similar, suggesting the promoting effects of HSR signal on chondrogenesis during bone-healing. In $G_{HSR1/2h}$, G_{HSR1h}, and G_{HSR3h}, the dose-dependent effect of HSR signal on chondrogenesis and bone mineralization was seen. With longer duration of daily PEMF treatment, cartilage formed earlier, in a larger quantity, and with more mineralized bone formation.

Our previous study,[30] and studies by other investigators,[34,35] demonstrated the enhancement of angiogenesis after PEMF treatment, suggesting that the HSR PEMF signal may promote cartilage formation and endochondral ossification via enhancing angiogenesis. Furthermore, the direct beneficial effects on chondrogenesis and cartilage hypertrophy by PEMF treatment have also been reported,[31,36] indicating that HSR PEMF signal may have direct effects on chondrogenesis, although the underlying mechanisms need further investigation.

The current study revealed that effects of PEMF were energy-specific. In comparison with the classic signal, the HSR signal is able to deliver a higher amount of energy per unit time to the injured site. Our results showed that this high-energy characteristic led to a remarkably shorter daily treatment duration while achieving similar healing outcomes. The energy-specific efficacy of PEMF was hypothesized and reported decades ago,[37] but the mechanisms are not yet fully understood. It is believed that by generating direct magnetic fields, as well as inducing electric currents in cells and the surrounding microenvironment, PEMF could cause free ions to move towards the electrodes and thereby affect the physiology of the cell,[38] which resembles mechanotransduction.[39] These ions such as calcium (Ca^{2+}), potassium (K^{+}), sodium (Na^{+}), and chlorine (Cl^{-}) serve as the first responders in translating the biophysical signal into a biological signal. The mechanism in energy transduction of PEMF was hypothesized as the oscillating PEMF would exert an oscillating force on each of the free ions, leading to a forced vibration.[40] When the amplitude of vibration transcends a certain threshold value, the oscillating ions may induce the electrically sensitive gating channels opening and ion flux, and therefore regulate the cellular functions.[41] Under this theory, the HSR signal could bring a stronger oscillating force, and lead to a larger scale of ion gating channels opening and ion flux, which may be responsible for the superior therapeutic outcome. Among these free ions, Ca^{2+} is considered as the prominent role of PEMF promotion effects on bone repair,[42] mainly due to its functions in excitable cells.[38] The activation of voltage-gated calcium channels (VGCCs) and influx of extracellular Ca^{2+} are both regulated by membrane depolarization, which could be induced by the time-varying electrical field formed by PEMF.[43,44] As the link between the non-thermal energy-related biophysical signal as PEMF, and the various

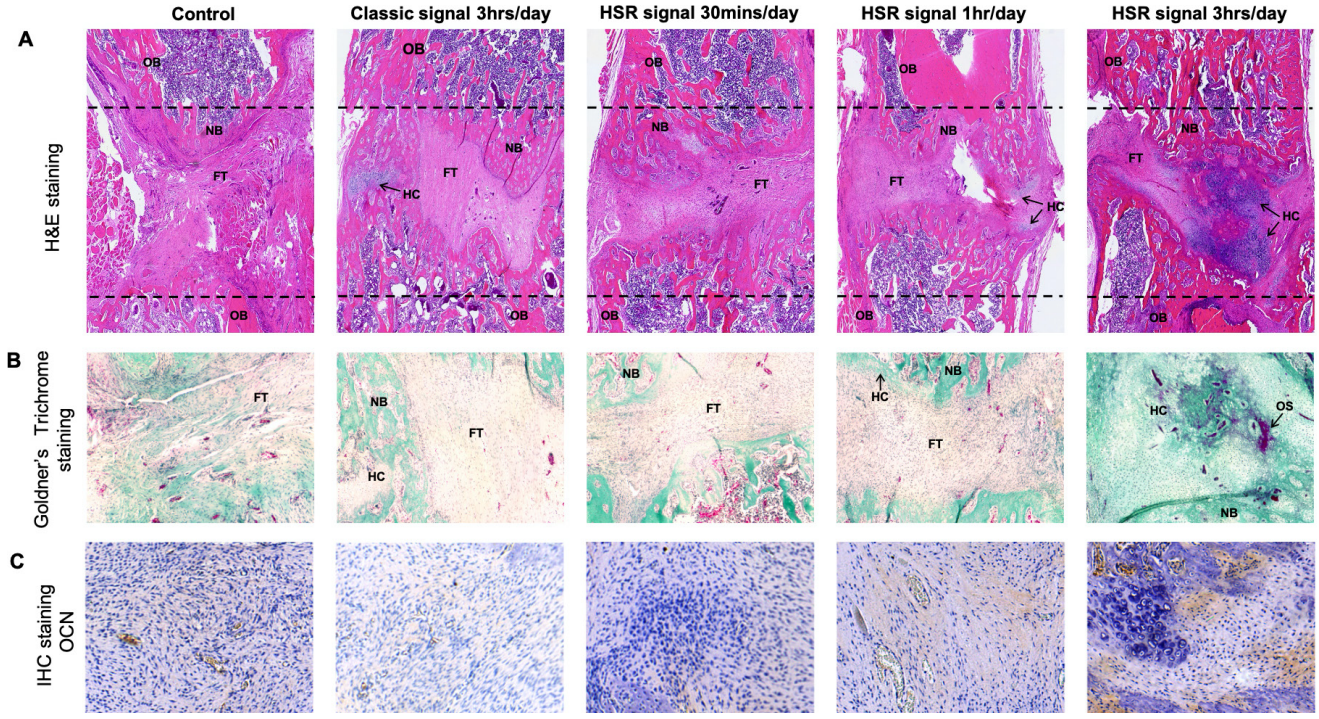

Fig. 6

Histological and immunohistochemical results of the distraction site on week 2 after distraction. a) Haematoxylin and eosin (H&E) staining of the distraction site. Each figure was obtained by collating 20 adjacent images of the distraction site (50× magnification). b) Goldner's Trichrome staining. Magnification: 50×. c) Immunohistochemistry (IHC) staining of osteocalcin (OCN). Magnification: 100×. FT: fibrous tissue; HC, hyaline cartilage; HSR, high slew rate; NB, new bone; OB, old bone; OS, osteoid.

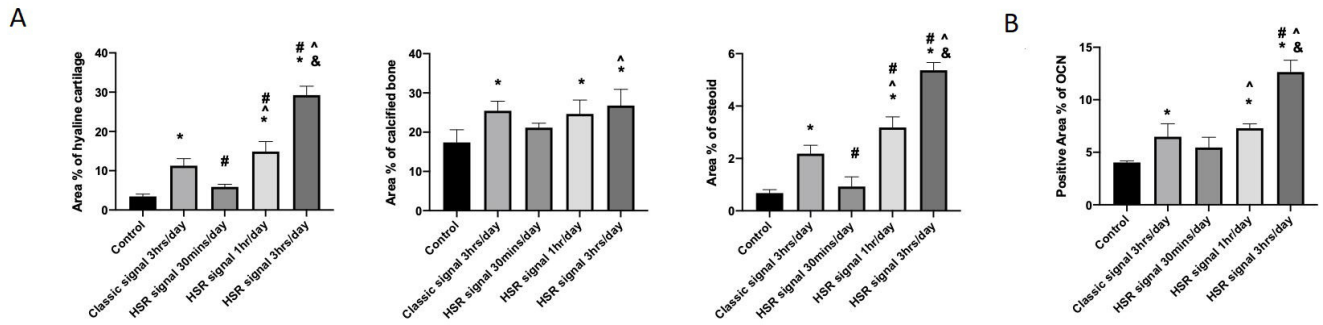

Fig. 7

a) Histomorphometric analysis was performed with images of Goldner's Trichrome staining using ImageJ (National Institutes of Health, USA). b) Semiquantitative analysis of immunohistochemical (IHC) staining was performed using ImageJ. Haematoxylin and eosin (H&E) and Goldner's Trichrome staining revealed that the bone formation was accelerated in GHSR3h, where a large amount of hyaline cartilage (HC) with some partially mineralized osteoid appeared within the distraction regenerate site. Whereas fibrous tissue was mostly observed in the distraction site in GHSR1/2h and Gcon, small amounts of hyaline cartilage were found inside the distraction regenerate site in Gclassic3h and GHSR1h. IHC staining of osteocalcin (OCN) indicated that all pulsed electromagnetic field (PEMF) treatments had different levels of promoting effects on OCN expression, and GHSR3h appeared to have the most increased expression of OCN. * vs control (Gcon), "#" vs classic signal three hrs/day (Gclassic3h), "^" vs HSR signal 30 mins/day (GHSR1/2h), "&" vs HSR signal one hr/day (GHSR1h), $p < 0.050$. One-way analysis of variance and Tukey's multi-comparison test were used for comparison of mean values. HSR, high slew rate.

biological effects caused by PEMF, the authors consider that the PEMF energy-specific effect could be initiated by different levels of forced movement of calcium and activation of VGCC, and consequently impact on calcium channel pathways and other signalling pathways. Furthermore, if the forced movement of calcium is the link between PEMF and regulation of cellular physiology, could calcium be an indicator to determine the 'windows' of the desirable PEMF parameters which may be more therapeutically effective?

The influences of PEMFs on bone and fracture healing are complex. Apart from the physiological characteristics involved in bone-healing,[45,46] PEMF parameters such as waveform, width of the pulse, frequency, duration, and intensity of exposure must be taken into account for proper clinical developments.[47] Efforts have been made

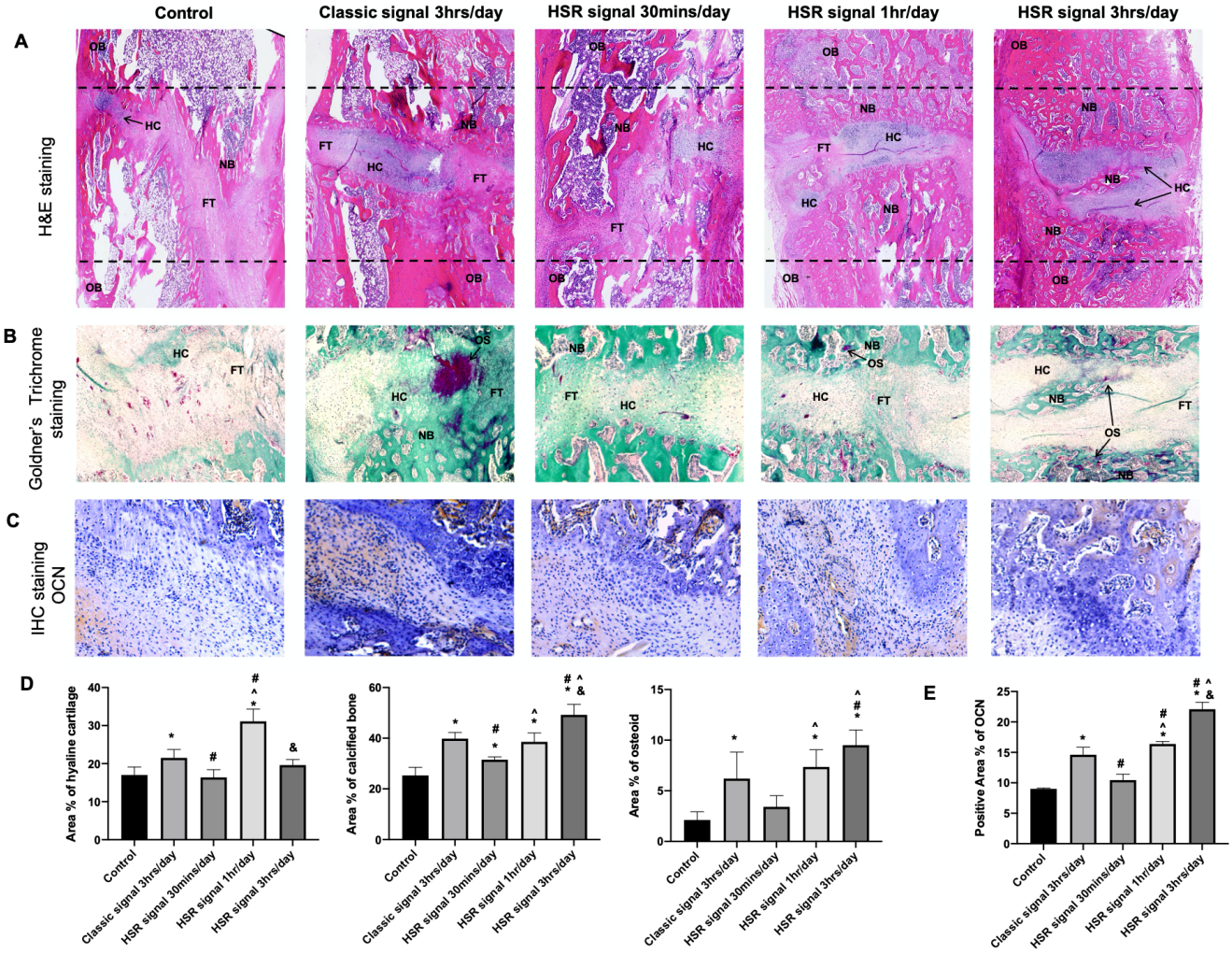

Fig. 8

Histological and immunohistochemical results of the distraction site on week 4 after distraction. a) Haematoxylin and eosin (H&E) staining of the distraction site. Each figure was obtained by stitching 20 adjacent images of the distraction site (50× magnification). b) Goldner's Trichrome staining. Magnification: 50×. c) Immunohistochemistry (IHC) staining of osteocalcin (OCN). Magnification: 100×. d) Histomorphometric analysis was performed with images of Goldner's Trichrome staining using ImageJ (National Institutes of Health, USA). e) Semiquantitative analysis of IHC staining was performed using ImageJ. H&E and Goldner's Trichrome staining showed that GHSR3h remained the best healing outcome with a significantly increased amount of calcified bone and a decreased percentage of hyaline cartilage compared to other groups. In GHSR1/2h and Gcon, a large amount of fibrous tissues still remained inside the bone defect site, whereas most of the soft-tissues had been replaced by hyaline cartilage in Gclassic3h and GHSR1h. The expression of OCN remained similar as GHSR3h still had the most abundant OCN expression in the distraction regenerate site. * vs control (Gcon), "#" vs classic signal hrs/day (Gclassic3h), "^" vs HSR signal 30 mins/day (GHSR1/2h), "&" vs HSR signal hr/day (GHSR1h), $p < 0.050$. One-way analysis of variance and Tukey's multi-comparison test were used for comparison of mean values. FT, fibrous tissue; HC, hyaline cartilage; HSR, high slew rate; NB, new bone; OB, old bone; OS, osteoid.

by different groups to determine the 'effect window', uncover the mechanisms, and seek criteria for the application of PEMFs. Previously, Ehnert et al[48] identified a specific extremely low frequency (ELF) PEMF that primary human osteoblasts were responsive to exposure via ERK1/2 activation. By comparing ten different defined ELF-PEMFs, the authors selected one signal with a frequency of 16 Hz, which appeared to be most effective in inducing proliferation and differentiation of human osteoblasts; they later uncovered that this signal could cause antioxidative defense mechanisms in human osteoblasts via induction of $\bullet O_2^-$ and H_2O_2.[49] Afterwards, this signal was proven by a randomized clinical trial to speed up osseous consolidation after high tibial osteotomy, especially for patients aged over 50 years.[50] In our study, we optimized our FDA-approved and clinically used signal into a HSR signal, and uncovered stronger beneficial effects on bone-healing. With more effects, we shall identify the underlying mechanism of this signal, and confirm its therapeutic potential on bone-healing with randomized clinical trials. As stated before, selecting the parameters likely to have maximum benefits in PEMF therapy is important for the optimization of clinical developments, and yet PEMFs may influence bone-healing through a variety of different pathways. We trust that through the combined endeavour from different groups, we will reach a consensus on PEMF therapy with optimal parameters and protocols for augmenting bone formation.

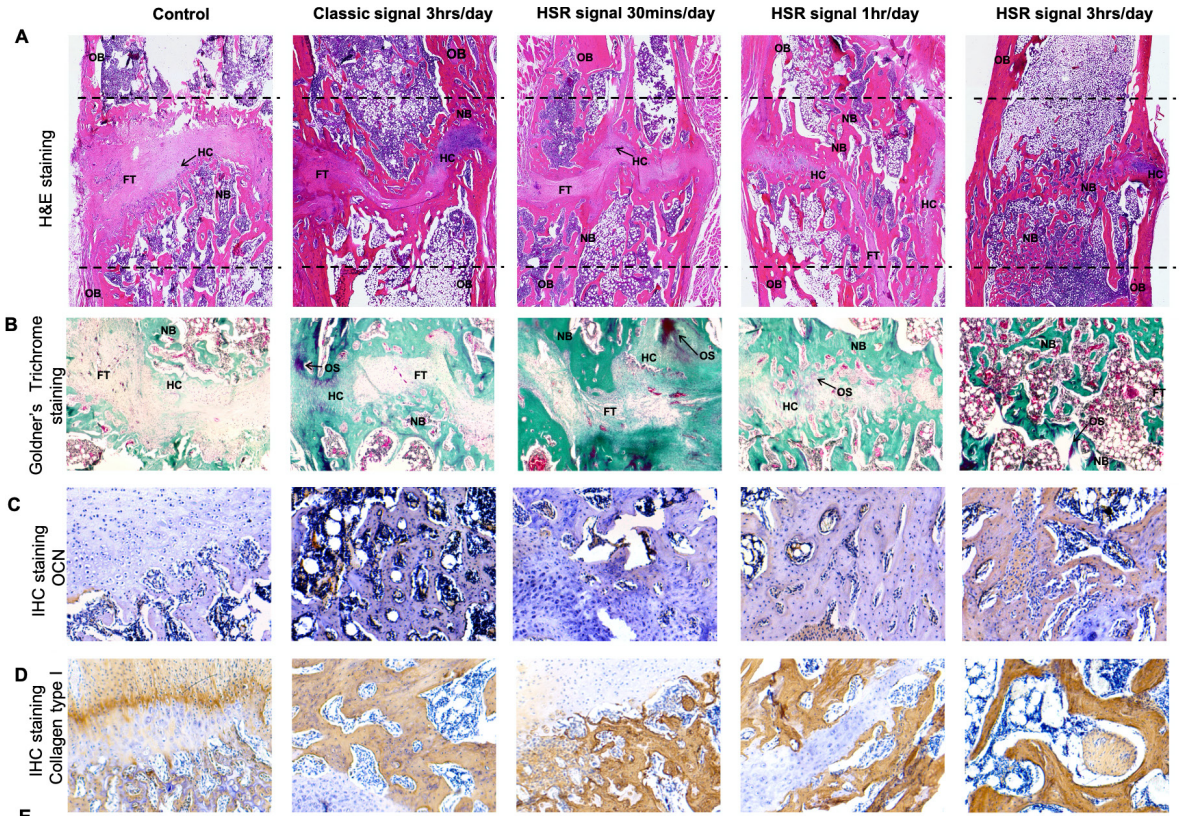

Fig. 9

Histological and immunohistochemical results of the distraction site on week 6 after distraction. a) Haematoxylin and eosin (H&E) staining of the distraction site.Each figure was obtained by stitching 20 adjacent images of the distraction site (50× magnification). b) Goldner's Trichrome staining. Magnification: 50×. c) Immunohistochemical (IHC) staining of osteocalcin (OCN). Magnification: 100×. d) IHC staining of collagen type I (Col I). FT, fibrous tissue; HC, hyaline cartilage; HSR, high slew rate; NB, new bone; OB, old bone; OS, osteoid.

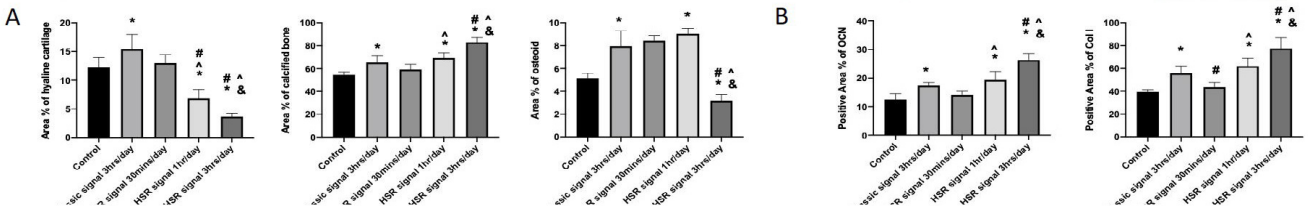

Fig. 10

a) Histomorphometric analysis was performed with images of Goldner's Trichrome staining using ImageJ (National Institutes of Health, USA). b) Semiquantitative analysis of immunohistochemical (IHC) staining was performed using ImageJ. Haematoxylin and eosin (H&E) and Goldner's Trichrome staining showed that in GHSR3h, endochondral ossification was mostly complete and bone-remodelling was partially complete, whereas in Gcon, Gclassic3h, GHSR1/2h, and GHSR1h, endochondral ossification and callus formation in the middle of the distraction regenerate were still ongoing, with signs of bone-remodelling. IHC staining of osteocalcin (OCN) indicated that OCN expression was still strong in Gclassic3h, GHSR1h, and GHSR3h. The highest expression level of collagen type I (Col I) was seen in GHSR3h, indicating that the best quality of new bone formation was achieved. * vs control (Gcon), "#" vs classic signal three hrs/day (Gclassic3h), "^" vs high slew rate (HSR) signal 30 mins/day (GHSR1/2h), "&" vs HSR signal one hr/day (GHSR1h), $p < 0.050$. One-way analysis of variance and Tukey's multi-comparison test were used for comparison of mean values.

Despite these encouraging findings, limitations remain in the current study. Firstly, despite the fact that the rat DO model has been well established and used for many studies, it may not reflect the actual clinical situation of DO. Bone formation is relatively faster in healthy rats, and therefore the study window is rather narrow. The use of unilateral external fixator/lengthener produces stress-shielding effects on the fixator attachment site, which we consider a systemic error that applies to all experimental animals. Secondly, despite the intriguing outcomes shown for HSR PEMF treatment group, further research is needed for mechanistic studies. Future research endeavours should focus on understanding how chondrogenesis, angiogenesis, and osteogenesis are connected under the influence of HSR PEMF, to develop more effective yet user-friendly PEMF protocols for clinical applications.

In conclusion, our data confirmed that HSR PEMF signal produces stronger promoting effects on chondrogenesis

and bone mineralization than that of a classic PEMF signal during DO in a rat model. The HSR signal could enhance bone formation and shorten the treatment duration in DO it may become a new PEMF clinical choice for patients undergoing DO treatments.

Supplementary material

An ARRIVE checklist is included to show that the ARRIVE guidelines were adhered to in this study.

References

1. **Ilizarov GA**. The tension-stress effect on the genesis and growth of tissues. Part I. The influence of stability of fixation and soft-tissue preservation. *Clin Orthop Relat Res*. 1989;238:249–281.
2. **Carvalho RS**, **Einhorn TA**, **Lehmann W**, **et al**. The role of angiogenesis in a murine tibial model of distraction osteogenesis. *Bone*. 2004;34(5):849–861.
3. **Lee DY**, **Cho T. J**, **Lee HR**, **et al**. Distraction osteogenesis induces endothelial progenitor cell mobilization without inflammatory response in man. *Bone*. 2010;46(3):673–679.
4. **Chappell TM**, **Ebert CC**, **McCann KM**, **Hutchinson BL**, **Rodriguez-Collazo E**. Distal tibial distraction osteogenesis-an alternative approach to addressing limb length discrepancy with concurrent hindfoot and ankle reconstruction. *J Orthop Surg Res*. 2019;14(1):244.
5. **Borzunov DY**, **Kolchin SN**, **Malkova TA**. Role of the Ilizarov non-free bone plasty in the management of long bone defects and nonunion: Problems solved and unsolved. *World J Orthop*. 2020;11(6):304–318.
6. **Zhang Q**, **Zhang W**, **Zhang Z**, **et al**. Femoral nonunion with segmental bone defect treated by distraction osteogenesis with monolateral external fixation. *J Orthop Surg Res*. 2017;12(1):183.
7. **Pacicca DM**, **Patel N**, **Lee C**, **et al**. Expression of angiogenic factors during distraction osteogenesis. *Bone*. 2003;33(6):889–898.
8. **Xu J**, **Wu T**, **Sun Y**, **et al**. Staphylococcal enterotoxin C2 expedites bone consolidation in distraction osteogenesis. *J Orthop Res*. 2017;35(6):1215–1225.
9. **Wang Y**, **Wan C**, **Szöke G**, **Ryaby JT**, **Li G**. Local injection of thrombin-related peptide (TP508) in PPF/PLGA microparticles-enhanced bone formation during distraction osteogenesis. *J Orthop Res*. 2008;26(4):539–546.
10. **Sun Y**, **Xu J**, **Xu L**, **et al**. MiR-503 Promotes Bone Formation in Distraction Osteogenesis through Suppressing Smurf1 Expression. *Sci Rep*. 2017;7(1):409.
11. **Xu J**, **Wang B**, **Sun Y**, **et al**. Human fetal mesenchymal stem cell secretome enhances bone consolidation in distraction osteogenesis. *Stem Cell Res Ther*. 2016;7(1):134.
12. **Sunay O**, **Can G**, **Cakir Z**. Autologous rabbit adipose tissue-derived mesenchymal stromal cells for the treatment of bone injuries with distraction osteogenesis. *Cytotherapy*. 2013;15(6):690–702.
13. **Canè V**, **Botti P**, **Soana S**. Pulsed magnetic fields improve osteoblast activity during the repair of an experimental osseous defect. *J Orthop Res*. 1993;11(5):664–670.
14. **Midura RJ**, **Ibiwoye MO**, **Powell KA**, **et al**. Pulsed electromagnetic field treatments enhance the healing of fibular osteotomies. *J Orthop Res*. 2005;23(5):1035–1046.
15. **De Haas WG**, **Lazarovici MA**, **Morrison DM**. The effect of low frequency magnetic fields on the healing of the osteotomized rabbit radius. *Clin Orthop Relat Res*. 1979;NA;(145):245.
16. **Grace KL**, **Revell WJ**, **Brookes M**. The effects of pulsed electromagnetism on fresh fracture healing: osteochondral repair in the rat femoral groove. *Orthopedics*. 1998;21(3):297–302.
17. **Ibiwoye MO**, **Powell KA**, **Grabiner MD**, **et al**. Bone mass is preserved in a critical-sized osteotomy by low energy pulsed electromagnetic fields as quantitated by in vivo micro-computed tomography. *J Orthop Res*. 2004;22(5):1086–1093.
18. **Inoue N**, **Ohnishi I**, **Chen D**, **Deitz LW**, **Schwardt JD**, **Chao EYS**. Effect of pulsed electromagnetic fields (PEMF) on late-phase osteotomy gap healing in a canine tibial model. *J Orthop Res*. 2002;20(5):1106–1114.
19. **de Haas WG**, **Watson J**, **Morrison DM**. Non-invasive treatment of ununited fractures of the tibia using electrical stimulation. *J Bone Joint Surg Br*. 1980;62-B(4):465–470.
20. **Sharrard WJ**, **Sutcliffe ML**, **Robson MJ**, **Maceachern AG**. The treatment of fibrous non-union of fractures by pulsing electromagnetic stimulation. *J Bone Joint Surg Br*. 1982;64-B(2):189–193.
21. **Shi H**, **Xiong J**, **Chen Y**, **et al**. Early application of pulsed electromagnetic field in the treatment of postoperative delayed union of long-bone fractures: a prospective randomized controlled study. *BMC Musculoskelet Disord*. 2013;14(1):35.
22. **Simonis RB**, **Parnell EJ**, **Ray PS**, **Peacock JL**. Electrical treatment of tibial non-union: a prospective, randomised, double-blind trial. *Injury*. 2003;34(5):357–362.
23. **Barker A**, **Dixon R**, **Sharrard W**, **Sutcliffe M**. Pulsed magnetic field therapy for tibial non-union: interim results of a double-blind trial. *Lancet*. 1984;323(8384):994–996.
24. **Bassett CA**, **Mitchell SN**, **Gaston SR**. Treatment of ununited tibial diaphyseal fractures with pulsing electromagnetic fields. *J Bone Joint Surg Am*. 1981;63-A(4):511–523.
25. **De Haas WG**, **Beaup A**, **Cameron H**, **English E**. The Canadian experience with pulsed magnetic fields in the treatment of ununited tibial fractures. *Clin Orthop Relat Res*. 1986;208:55–58.
26. **Gupta AK**, **Srivastava KP**, **Avasthi S**. Pulsed electromagnetic stimulation in nonunion of tibial diaphyseal fractures. *Indian J Orthop*. 2009;43(2):156–160.
27. **Tsai M-T**, **Li W-J**, **Tuan RS**, **Chang WH**. Modulation of osteogenesis in human mesenchymal stem cells by specific pulsed electromagnetic field stimulation. *J Orthop Res*. 2009;27(9):1169–1174.
28. **Ongaro A**, **Pellati A**, **Bagheri L**, **Fortini C**, **Setti S**, **De Mattei M**. Pulsed electromagnetic fields stimulate osteogenic differentiation in human bone marrow and adipose tissue derived mesenchymal stem cells. *Bioelectromagnetics*. 2014;35(6):426–436.
29. **Pan Y**, **Dong Y**, **Hou W**, **et al**. Effects of PEMF on microcirculation and angiogenesis in a model of acute hindlimb ischemia in diabetic rats. *Bioelectromagnetics*. 2013;34(3):180–188.
30. **Li Y**, **Pan Q**, **Zhang N**, **et al**. A novel pulsed electromagnetic field promotes distraction osteogenesis via enhancing osteogenesis and angiogenesis in a rat model. *Journal of Orthopaedic Translation*. 2020;25:87–95.
31. **Zhang B**, **Xie Y**, **Ni Z**, **Chen L**. Effects and Mechanisms of Exogenous Electromagnetic Field on Bone Cells: A Review. *Bioelectromagnetics*. 2020;41(4):263–278.
32. **Androjna C**, **Yee CS**, **White CR**, **et al**. A comparison of alendronate to varying magnitude PEMF in mitigating bone loss and altering bone remodeling in skeletally mature osteoporotic rats. *Bone*. 2021;143:115761.
33. **Garland DE**, **Moses B**, **Salyer W**. Long-term follow-up of fracture nonunions treated with PEMFs. *Contemp Orthop*. 1991;22(3):295–302.
34. **Tepper OM**, **Callaghan MJ**, **Chang EI**, **et al**. Electromagnetic fields increase in vitro and in vivo angiogenesis through endothelial release of FGF-2. *FASEB J*. 2004;18(11):1231–1233.
35. **Delle Monache S**, **Alessandro R**, **Iorio R**, **Gualtieri G**, **Colonna R**. Extremely low frequency electromagnetic fields (ELF-EMFs) induce in vitro angiogenesis process in human endothelial cells. *Bioelectromagnetics*. 2008;29(8):640–648.
36. **Norton LA**, **Witt DW**, **Rovetti LA**. Pulsed electromagnetic fields alter phenotypic expression in chondroblasts in tissue culture. *J Orthop Res*. 1988;6(5):685–689.
37. **Rubin CT**, **Donahue HJ**, **Rubin JE**, **McLeod KJ**. Optimization of electric field parameters for the control of bone remodeling: exploitation of an indigenous mechanism for the prevention of osteopenia. *J Bone Miner Res*. 2009;8(S2):S573–S581.
38. **Wade B**. A Review of Pulsed Electromagnetic Field (PEMF) Mechanisms at a Cellular Level: A Rationale for Clinical Use. *AJHR*. 2013;1(3):51–55.
39. **Stewart S**, **Darwood A**, **Masouros S**, **Higgins C**, **Ramasamy A**. Mechanotransduction in osteogenesis. *Bone Joint Res*. 2020;9(1):1–14.
40. **Panagopoulos DJ**, **Karabarbounis A**, **Margaritis LH**. Mechanism for action of electromagnetic fields on cells. *Biochem Biophys Res Commun*. 2002;298(1):95–102.
41. **Panagopoulos DJ**, **Messini N**, **Karabarbounis A**, **Philippetis AL**, **Margaritis LH**. A Mechanism for Action of Oscillating Electric Fields on Cells. *Biochem Biophys Res Commun*. 2000;272(3):634–640.
42. **Pall ML**. Electromagnetic fields act via activation of voltage-gated calcium channels to produce beneficial or adverse effects. *J Cell Mol Med*. 2013;17(8):958–965.
43. **Yuan J**, **Xin F**, **Jiang W**. Underlying signaling pathways and therapeutic applications of pulsed electromagnetic fields in bone repair. *Cell Physiol Biochem*. 2018;46(4):1581–1594.
44. **Li Y**, **Yan X**, **Liu J**, **et al**. Pulsed electromagnetic field enhances brain-derived neurotrophic factor expression through L-type voltage-gated calcium channel- and Erk-dependent signaling pathways in neonatal rat dorsal root ganglion neurons. *Neurochem Int*. 2014;75:96–104.
45. **Starlinger J**, **Kaiser G**, **Thomas A**, **Sarahrudi K**. The impact of nonosteogenic factors on the expression of osteoprotegerin and RANKL during human fracture healing. *Bone Joint Res*. 2019;8(7):349–356.
46. **Chow SK-H**, **Chim Y-N**, **Wang J-Y**, **Wong RM-Y**, **Choy VM-H**, **Cheung W-H**. flammatory response in postmenopausal osteoporotic fracture healing. *Bone Joint Res*. 2020;9(7):368–385.

47. **Daish C**, **Blanchard R**, **Fox K**, **Pivonka P**, **Pirogova E**. The application of pulsed electromagnetic fields (PEMFs) for bone fracture repair: past and perspective findings. *Ann Biomed Eng*. 2018;46(4):525–542.
48. **Ehnert S**, **Falldorf K**, **Fentz A-K**, **et al**. Primary human osteoblasts with reduced alkaline phosphatase and matrix mineralization baseline capacity are responsive to extremely low frequency pulsed electromagnetic field exposure - Clinical implication possible. *Bone Rep*. 2015;3:48–56.
49. **Ehnert S**, **Fentz A-. K**, **Schreiner A**, **et al**. Extremely low frequency pulsed electromagnetic fields cause antioxidative defense mechanisms in human osteoblasts via induction of •O2- and H2O2. *Sci Rep*. 2017;7(1):14544.
50. **Ziegler P**, **Nussler AK**, **Wilbrand B**, **et al**. Pulsed Electromagnetic Field Therapy Improves Osseous Consolidation after High Tibial Osteotomy in Elderly Patients-A Randomized, Placebo-Controlled, Double-Blind Trial. *J Clin Med*. 2019;8(11):2008.

Author information:
- Y. Li, MBBS, PhD, Postdoctoral Fellow
- Y. Yang, MBBS, PhD Student
- M. Wang, MBBS, PhD Student
- X. Zhang, MSc, PhD Candidate
- S. Bai, MBBS, PhD Candidate
- X. Lu, MBBS, PhD Student
- Y. Li, MPhil, PhD Candidate
- G. Li, MBBS, D Phil (Oxon), Professor
  Department of Orthopaedic and Traumatology, Faculty of Medicine, The Chinese University of Hong Kong, Hong Kong, China; Stem Cells and Regenerative Medicine Laboratory, Li Ka Shing Institute of Health Sciences, The Chinese University of Hong Kong, Prince of Wales Hospital, Hong Kong, China.
- E. I. Waldorff, PhD, Principal Scientist and Research Manager
- N. Zhang, PhD, Principal Scientist and Pre-Clinical Research Manager
  Research & Clinical Affairs, Orthofix Medical Inc, Lewisville, Texas, USA.
- W. Y-W. Lee, PhD, Assistant Professor, Department of Orthopaedic and Traumatology, Faculty of Medicine, The Chinese University of Hong Kong, Hong Kong, China; SH Ho Scoliosis Research Laboratory, Joint Scoliosis Research Center of the Chinese University of Hong Kong and Nanjing University, Department of Orthopaedics and Traumatology, The Chinese University of Hong Kong, Hong Kong, China; Li Ka Shing Institute of Health Sciences, The Chinese University of Hong Kong, Hong Kong, China.

Author contributions:
- Y. Li: Investigation, Methodology, Data curation, Writing – original draft.
- Y. Yang: Investigation, Data curation, Writing – original draft.
- M. Wang: Investigation, Validation.
- X. Zhang: Methodology, Investigation.
- S. Bai: Methodology, Investigation.
- X. Lu: Methodology, Investigation.
- Y. Li: Methodology, Investigation.
- E. I. Waldorff: Methodology, Validation, Software, Writing – review & editing.
- N. Zhang: Methodology, Validation, Software, Writing – review & editing.
- W. Y. Lee: Methodology, Supervision, Writing – review & editing.
- G. Li: Conceptualization, Methodology, Supervision, Writing – review & editing.

- Y. Li and Y. Yang contributed equally to this work.

Funding statement:
- The author or one or more of the authors have received or will receive benefits for personal or professional use from a commercial party related directly or indirectly to the subject of this article.

ICMJE COI statement:
- The authors have no conflicts of interest to disclose in relation to this article. NZ and EIW are employees of and own stock in Orthofix Medical Inc. This work was also partially supported by CUHK Direct Grant (Ref No: 2019.055).

Acknowledgements:
- The authors would like to thank Orthofix Medical Inc. for providing the PEMF devices and their technical support.

Open access funding
- The authors confirm that the open access fee was funded by Orthofix Medical Inc.